Electronic Supplementary Material (ESI) for ChemComm.

Electronic Supporting Information

All-Atom Lipid Bilayer Self-Assembly with the AMBER and Charmm Lipid Force Fields

Å. A. Skjevik,[a,b] B. D. Madej,[a,d] C. J. Dickson,[c] K. Teigen,[b] R. C. Walker [a,d,*] and I. R. Gould[c,*]

[a] San Diego Supercomputer Center, University of California San Diego, 9500 Gilman Drive MC0505, La Jolla, California, 92093-0505, United States.

[b] Department of Biomedicine, University of Bergen, N-5009 Bergen, Norway.

[c] Department of Chemistry and Institute of Chemical Biology, Imperial College London, South Kensington, SW7 2AZ, United Kingdom.

[d] Department of Chemistry and Biochemistry, University of California San Diego, 9500 Gilman Drive MC0505, La Jolla, California, 92093-0505, United States.

CONTENTS

METHODS

Simulation details. All simulations were run using the GPU/CUDA-accelerated implementation of AMBER PMEMD (Version 14.0)[1, 2] from AMBER 14[3, 4]. Periodic boundary conditions were applied, with the electrostatic interactions evaluated by means of particle mesh Ewald (PME) summation[5] with 4th order B-spline interpolation and grid spacings of 1.0 Å. A cut-off of 10 Å limited the direct space sum and truncated the van der Waals interactions. Bonds involving hydrogen were subjected to length constraints provided by the SHAKE algorithm[6]. The Langevin coupling scheme[7], with a collision frequency of 1.0 ps^{-1}, regulated temperature while a Berendsen barostat[8] maintained a reference pressure set to 1.0 bar. All simulations utilized the hybrid SPFP precision model of Le Grand and Walker[9].

Self-assembly simulations. Three repeats with Lipid14 parameters were conducted for each of the four lipid systems in Supporting Table 1 (POPC, DOPC, POPE and DPPC), starting from the same initial random configuration of lipid, water and ions, but using different random seeds for each repeat. After a 10,000-step minimization, the following simulation protocol was followed: i) 10 ns simulation at production temperature with 0.5 fs time step and isotropic pressure coupling (NPT) using initial velocities generated from a Boltzmann distribution; ii) 10 ns simulation at production temperature with 1.0 fs time step and isotropic pressure coupling (NPT); iii) Simulation at production temperature with 2.0 fs time step and anisotropic pressure coupling (NPT). The production temperature was maintained across all three steps, above the phase transition temperature of the simulated phospholipid (see Supporting Table 1 for specific temperatures). The simulation parameters applied in step iii) are identical to those used in the production phase of the Lipid14 parameter validation simulations[10].

Equivalent systems as listed in Supporting Table 1, with the same number of lipids, waters and ions, were generated with the Charmm C36 force field[11] and converted to AMBER topology and coordinate files using CHAMBER[12]. In three simulation repeats per lipid, the same procedure as for the Lipid14 systems was followed and the same simulation settings applied.

Trajectory analyses. Since asymmetric lipid distribution was observed in most of the simulations (Table 1) the areas per lipid were calculated by doubling the lateral area of the assembled bilayer and dividing by the total number of phospholipids in the system. The volume per lipid (V_L) was derived using the volume of the simulation box (V_{box}), the number of water (n_w) and lipid (n_{lipid}) molecules and the temperature-specific volume of a TIP3P water molecule (V_w)[10, 13]:

$$V_L = \frac{V_{box} - n_w V_w}{n_{lipid}}$$

Bilayer thickness (D_{HH}) was obtained as the distance between the maxima (i.e. the phosphate peaks) of the time-averaged electron density profile, while the Luzzati thickness was calculated by subtracting the integral of the water density probability distribution ($\rho_w(bn)$) along the bilayer normal dimension (bn) from the time-averaged bilayer normal dimension d_{bn}[10, 14, 15]:

$$D_B = d_{bn} - \int_{-d_{bn}/2}^{d_{bn}/2} \rho_w(bn) d_{bn}$$

Isothermal compressibility moduli (K_A) were obtained through the following equation[10, 13]:

$$K_A = \frac{2k_B T \left\langle A_L \right\rangle}{n_{lipid} \sigma_A^{\,2}}$$

T is the temperature, k_B is the Boltzmann constant, $<A_L>$ refers to the mean area per lipid and σ_A^2 corresponds to the area per lipid variance.

The lateral diffusion coefficient (D) was computed as the slope of the plot of the mean square displacement (*MSD*) of the lipids versus time t (the number of dimensions, n, is equal to 2 for lateral diffusion in bilayers):

$$D = \lim_{t\to\infty} \frac{MSD}{2nt}$$

Any centre of mass drift of each bilayer leaflet was removed from the trajectories before calculating the average *MSD* over a large number of 20 ns windows of different time origin, with 200 ps separating the time origins of sequentially analyzed windows. The last 100 ns of each simulation was used for the *MSD* calculation, and the linear 10-20 ns portion of the resulting curve was used for deriving the slope via linear regression[10].

The bulk of the analyses described above was carried out using PTRAJ/CPPTRAJ[3, 16], and the snapshots in Figure 1 were generated using VMD[17].

SUPPORTING TABLES

Supporting Table 1: Simulation system details

System	Number of lipids	TIP3P water/lipid ratio n_w	Number of K^+/Cl^-	Simulation time per repeat (ns)[a]	Simulation temperature (K)
DOPC	128	32.8	12/12	1,000	303.0
POPC	128	31.0	11/11	1,000	303.0
POPE	128	32.0	12/12	1,000	310.0
DPPC	128	30.1	11/11	1,000	323.0

[a] Three simulation repeats (1 μs each) were conducted for each system, both with Lipid14 parameters and Charmm C36 parameters.

Supporting Table 2: Additional average structural properties calculated for the self-assembled Lipid14 and C36 bilayers and comparison with experiment

Lipid	Simulation number	Bilayer formation time (ns)[a]		Volume per lipid (Å^3)[b]			Bilayer thickness D_{HH} (Å)[b]			Luzzati thickness D_B (Å)[b]		
		Lipid14	*C36*	*Lipid14*	*C36*	*Exp.*	*Lipid14*	*C36*	*Exp.*	*Lipid14*	*C36*	*Exp.*
DOPC	1	150	135	1251.5 ± 4.4	1238.1 ± 4.2	1303[18]	37.25	38	35.3[19], 36.7[20], 36.9[18], 37.1[21]	36.2	36.5	35.9[18], 36.1[21], 38.7[20]
	2	285	145	1251.5 ± 4.4	1238.1 ± 4.2		37	38.25		36.2	36.5	
	3	720	160	1251.3 ± 4.4	1238.1 ± 4.2		37.5	37.5		36.3	36.6	
POPC	1	375	160	1207.3 ± 4.3	1191.9 ± 4.2	1256[22]	37.25	38	37[22]	36.9	37.4	36.8[22], 39.1[23]
	2	535	325	1207.4 ± 4.3	1191.7 ± 4.2		37.25	38.5		36.8	37.5	
	3	755	425	1207.1 ± 4.4	1191.9 ± 4.1		37.25	38.25		36.8	37.4	
POPE	1	70	95	1141.1 ± 4.4	1134.9 ± 4.3	1180[24]	42.25	40.75	39.5[24]	40.8	40.0	-
	2	100	115	1141.2 ± 4.5	1134.7 ± 4.5		42	41.5		40.5	40.2	
	3	125	205	1140.4 ± 4.8	1135.1 ± 4.3		41.5	41		39.9	39.9	
DPPC	1	230	35	1178.8 ± 5.1	1132.8 ± 24.8	1232[18]	38	40.25	38[20], 38.3[18]	38.0	39.8	39.0[23]
	2	350	85	1179.4 ± 4.9	1114.9 ± 20.1		37.75	43.75		37.9	41.7	
	3	440	325	1178.7 ± 5.0	1116.2 ± 20.3		37.75	42		37.9	40.3	

[a] Repeats listed in the same order as in Table 1

[b] Calculated from the interval from 50 ns after bilayer was fully formed until 1 μs of total simulation time. Due to an initial bilayer equilibration phase, the properties were calculated from the last 400 ns for the last Lipid14 DPPC repeat listed.

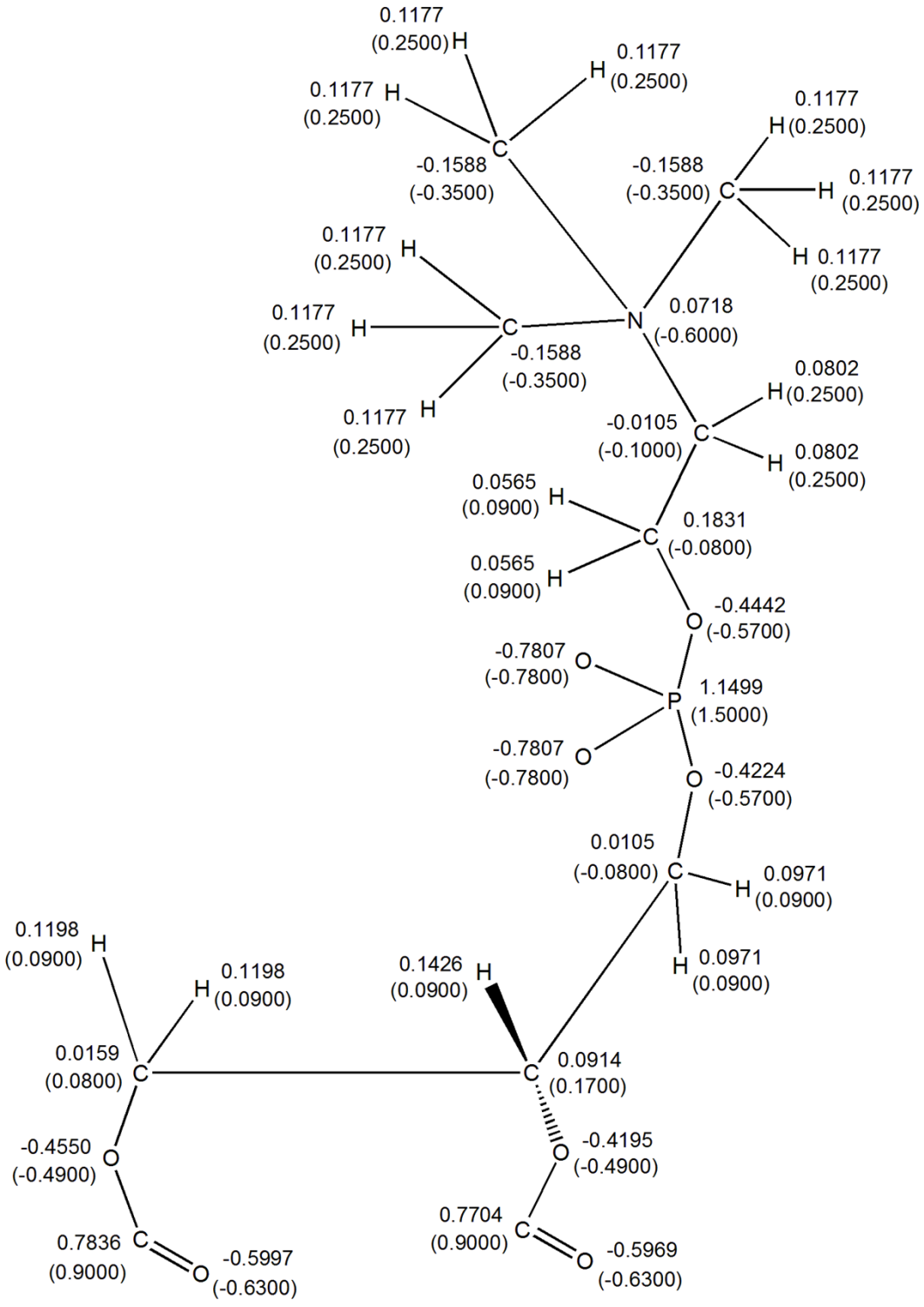

Supporting Figure 1. Atomic point charges in the PC head group in Lipid14 (taken from lipid14.lib) with corresponding C36 charges in parentheses (taken from top_all36_lipid.rtf).

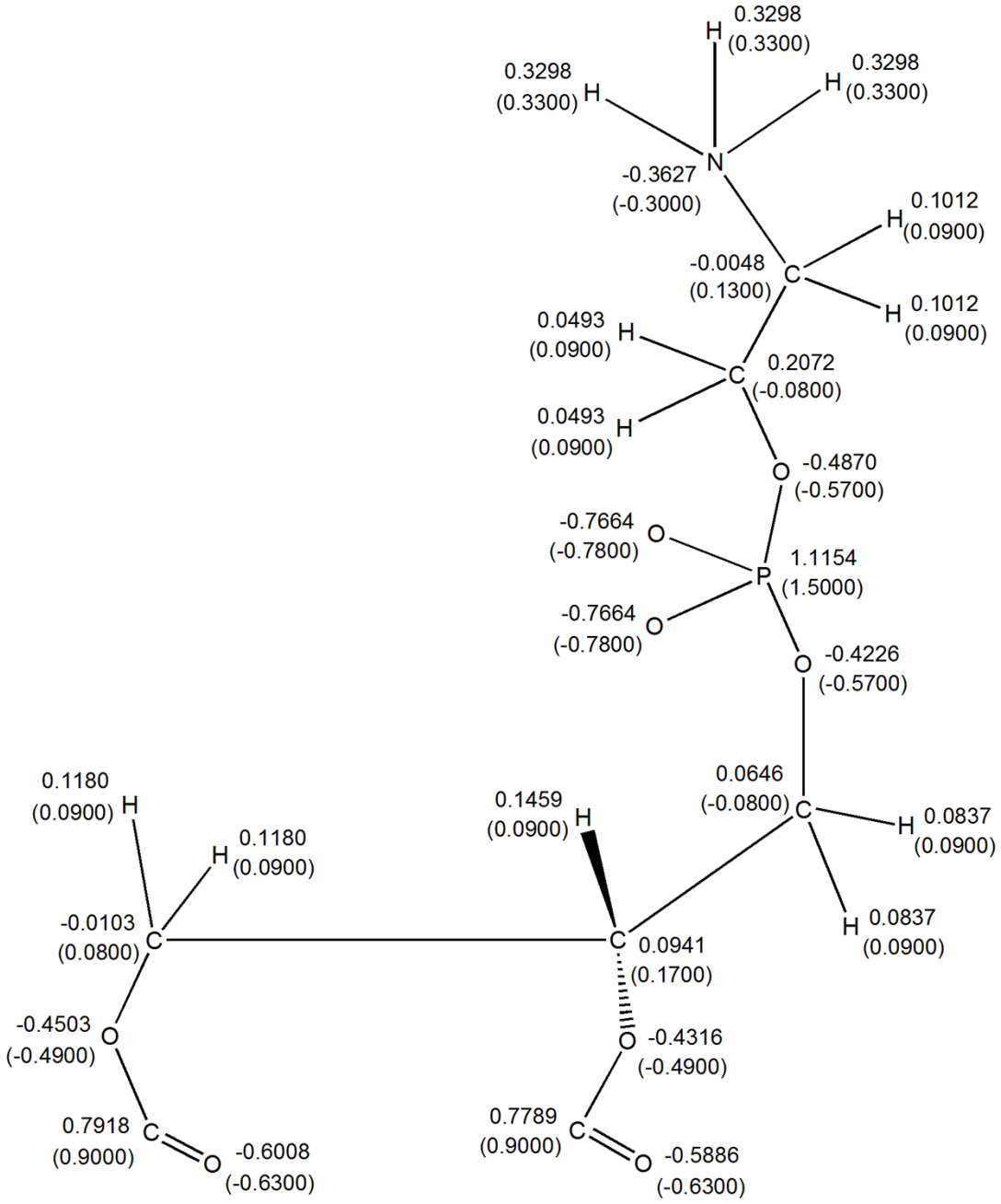

Supporting Figure 2. Atomic point charges in the PE head group in Lipid14 (taken from lipid14.lib) with corresponding C36 charges in parentheses (taken from top_all36_lipid.rtf).

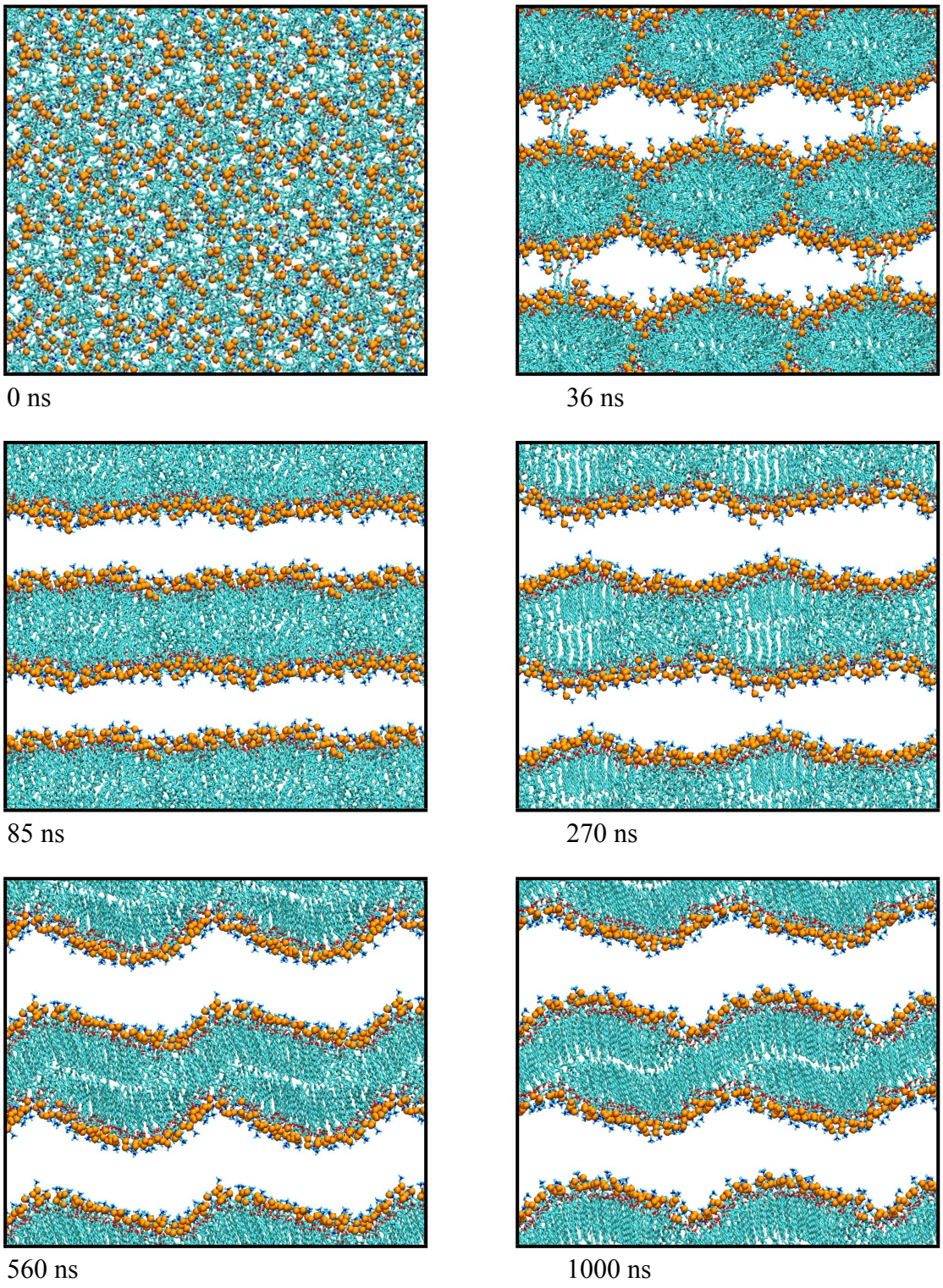

Supporting Figure 1. C36 DPPC self-assembly. The snapshots are taken from the first simulation listed in Table 1 and are representative of all three repeats (though with different timings). The lipids eventually adopt a highly ordered configuration, where tails from opposite leaflets completely overlap in parts of the membrane (after 560, 600 and 700 ns for the three repeats, respectively). This configuration is very stable for the remainder of the simulation.

CAPTIONS FOR SUPPORTING VIDEOS

Supporting Video 1: DOPC self-assembly. The video shows the first 250 ns of the first Lipid14 DOPC self-assembly simulation listed in Table 1, with a simulation time interval of 200 ps between frames. The lipids are represented as line models coloured by element, with the head group phosphorus atoms highlighted as orange spheres. Water, ions and hydrogens have been removed for clarity.

Supporting Video 2: POPC self-assembly. The video shows the first 475 ns of the first Lipid14 POPC self-assembly simulation listed in Table 1, with a simulation time interval of 200 ps between frames. The lipids are represented as line models coloured by element, with the head group phosphorus atoms highlighted as orange spheres. Water, ions and hydrogens have been removed for clarity.

Supporting Video 3: POPE self-assembly. The video shows the first 200 ns of the second Lipid14 POPE self-assembly simulation listed in Table 1, with a simulation time interval of 200 ps between frames. The lipids are represented as line models coloured by element, with the head group phosphorus atoms highlighted as orange spheres. Water, ions and hydrogens have been removed for clarity.

Supporting Video 4: DPPC self-assembly. The video shows the first 700 ns of the third Lipid14 DPPC self-assembly simulation listed in Table 1, with a simulation time interval of 200 ps between frames. The lipids are represented as line models coloured by element, with the head group phosphorus atoms highlighted as orange spheres. Water, ions and hydrogens have been removed for clarity.

REFERENCES

1. A. W. Götz, M. J. Williamson, D. Xu, D. Poole, S. Le Grand and R. C. Walker, *J. Chem. Theory Comput.*, 2012, **8**, 1542-1555.

2. R. Salomon-Ferrer, A. W. Götz, D. Poole, S. Le Grand and R. C. Walker, *J. Chem. Theory Comput.*, 2013, **9**, 3878-3888.

3. D. A. Case, V. Babin, J. T. Berryman, R. M. Betz, Q. Cai, D. S. Cerutti, T. E. Cheatham, III, T. A. Darden, R. E. Duke, H. Gohlke, A. W. Götz, S. Gusarov, N. Homeyer, P. Janowski, J. Kaus, I. Kolossváry, A. Kovalenko, T. S. Lee, S. Le Grand, T. Luchko, R. Luo, B. D. Madej, K. M. Merz, F. Paesani, D. R. Roe, A. Roitberg, C. Sagui, R. Salomon-Ferrer, G. Seabra, C. Simmerling, W. Smith, J. Swails, R. C. Walker, J. Wang, R. M. Wolf, X. Wu and P. A. Kollman, AMBER 14, University of California, San Francisco, 2014.

4. R. Salomon-Ferrer, D. A. Case and R. C. Walker, *WIREs Comput. Mol. Sci.*, 2013, **3**, 198-210.

5. T. Darden, D. York and L. Pedersen, *J. Chem. Phys.*, 1993, **98**, 10089-10092.

6. J.-P. Ryckaert, G. Ciccotti and H. J. C. Berendsen, *J. Comput. Phys.*, 1977, **23**, 327-341.

7. R. J. Loncharich, B. R. Brooks and R. W. Pastor, *Biopolymers*, 1992, **32**, 523-535.

8. H. J. C. Berendsen, J. P. M. Postma, W. F. van Gunsteren, A. DiNola and J. R. Haak, *J. Chem. Phys.*, 1984, **81**, 3684-3690.

9. S. Le Grand, A. W. Götz and R. C. Walker, *Comput. Phys. Commun.*, 2013, **184**, 374-380.

10. C. J. Dickson, B. D. Madej, Å. A. Skjevik, R. M. Betz, K. Teigen, I. R. Gould and R. C. Walker, *J. Chem. Theory Comput.*, 2014, **10**, 865-879.

11. J. B. Klauda, R. M. Venable, J. A. Freites, J. W. O'Connor, D. J. Tobias, C. Mondragon-Ramirez, I. Vorobyov, A. D. MacKerell, Jr. and R. W. Pastor, *J. Phys. Chem. B*, 2010, **114**, 7830-7843.

12. M. F. Crowley, M. J. Williamson and R. C. Walker, *Int. J. Quantum Chem.*, 2009, **109**, 3767-3772.

13. C. J. Dickson, L. Rosso, R. M. Betz, R. C. Walker and I. R. Gould, *Soft Matter*, 2012, **8**, 9617-9627.

14. J. P. M. Jämbeck and A. P. Lyubartsev, *J. Phys. Chem. B*, 2012, **116**, 3164-3179.

15. D. Poger, W. F. van Gunsteren and A. E. Mark, *J. Comput. Chem.*, 2010, **31**, 1117-1125.

16. D. R. Roe and T. E. Cheatham, III, *J. Chem. Theory Comput.*, 2013, **9**, 3084-3095.

17. W. Humphrey, A. Dalke and K. Schulten, *J. Mol. Graph.*, 1996, **14**, 33-38.

18. J. F. Nagle and S. Tristram-Nagle, *Biochim. Biophys. Acta*, 2000, **1469**, 159-195.

19. S. Tristram-Nagle, H. I. Petrache and J. F. Nagle, *Biophys. J.*, 1998, **75**, 917-925.

20. N. Kučerka, J. F. Nagle, J. N. Sachs, S. E. Feller, J. Pencer, A. Jackson and J. Katsaras, *Biophys. J.*, 2008, **95**, 2356-2367.

21. Y. Liu and J. F. Nagle, *Phys Rev E*, 2004, **69**, 040901.

22. N. Kučerka, S. Tristram-Nagle and J. F. Nagle, *J. Membr. Biol.*, 2005, **208**, 193-202.

23. N. Kučerka, M.-P. Nieh and J. Katsaras, *Biochim. Biophys. Acta*, 2011, **1808**, 2761-2771.

24. M. Rappolt, A. Hickel, F. Bringezu and K. Lohner, *Biophys. J.*, 2003, **84**, 3111-3122.